

# Lighthouse: An Open Research Framework for Optical Data Center Networks

Yiming Lei<sup>1</sup> Federico De Marchi<sup>1</sup> Jialong Li<sup>1</sup> Raj Joshi<sup>2</sup> Balakrishnan Chandrasekaran<sup>3</sup> Yiting Xia<sup>1</sup>

<sup>1</sup>Max Planck Institute for Informatics <sup>2</sup>Harvard University <sup>3</sup>Vrije Universiteit Amsterdam

## Abstract

Optical data center networks (DCNs) are emerging as a promising design for cloud infrastructure. However, existing optical DCN architectures operate as closed ecosystems, tying software solutions to specific optical hardware. We introduce Lighthouse, an open research framework that decouples software from hardware, allowing them to evolve independently. Central to Lighthouse is the time-flow table abstraction, serving as a common interface between optical hardware and software. We develop Lighthouse on programmable switches, achieving a minimum optical circuit duration of 2  $\mu$ s, the shortest duration realized by commodity devices to date. We demonstrate Lighthouse’s generality by implementing six optical architectures on an optical testbed and conducted extensive benchmarks on a 108-ToR setup, highlighting system efficiency. Additionally, we present case studies that identify potential research topics enabled by Lighthouse.

## 1 Introduction

In the post-Moore’s law era for merchant silicon, the networking community has turned to optical circuit switch (OCS) technologies for their power, cost, and bandwidth advantages. Numerous optical data center network (DCN) architectures have been proposed to build high-performance DCN fabrics with different *OCS hardware* [6, 10, 12–14, 16, 17, 19, 25, 28, 29, 31, 34, 35, 40, 41, 43–45].

However, OCSes are bufferless physical-layer devices transmitting only optical signals. As illustrated in Fig. 1, they establish exclusive optical circuits between Top-of-Rack switch (ToR) pairs and reconfigure the circuits forming varying network topologies. Hence, to make an optical DCN functional, a *software system* must coordinate packet buffering and scheduling on ToRs to align with the circuit availability.

The *tight coupling of optical hardware and software systems* makes research and innovation for optical DCNs siloed. Each optical DCN architecture is a *closed ecosystem* comprising specialized optical hardware and customized networked systems to support that hardware. System solutions are tied to the underlying hardware architecture, creating a high *barrier to entry* for system researchers with little optics expertise.

Equally tied to the optical architecture is the *experimental environment*. To date, most system designs for optical DCNs are evaluated on home-grown simulators for the specific architecture. The only end-to-end evaluation platform, Etalon [33], is limited to the electrical-optical hybrid architecture and emulates switches on hosts without the actual switch stack. The lack of realistic and general experimental environment makes

it extremely difficult to validate, compare, and improve different proposals, which further hinders the innovation cycle.

In this paper, we present Lighthouse, an open research framework to *decouple software systems from optical hardware, enabling them to evolve independently*. We aim to make Lighthouse a “narrow waist” for optical DCNs, building a general system stack that supports easy integration of various optical hardware downward and free exploration of network protocols upward. The key challenge is defining a *common interface* between hardware and software across diverse optical architectures. Like the IP layer in traditional networks, we believe this interface lies in routing, as the core function of the network is to direct traffic through the dynamic circuits.

Routing in traffic-aware (*TA*) architectures, the first generation of optical DCNs, is relatively straightforward, with some solutions already deployed in production [27, 35]. These architectures collect traffic statistics to establish on-demand circuits for communication hot spots [14, 16, 17, 25, 26, 34, 40] or optimize the topology periodically based on long-term traffic patterns [12, 13, 27, 35, 45]. Routing happens within each topology instance of circuit configuration like in static networks, thus route updates upon topology change can be handled via standard SDN methods, updating flow table entries and falling back to default routes during circuit disruptions.

The recent traffic-oblivious (*TO*) architectures are significantly more complex. Using the latest OCS technologies, they reconfigure circuits in microsecond or even sub-microsecond intervals, known as time slices, to approach packet-level reconfiguration similar to electrical networks [6, 10, 23, 24, 29, 31]. At this granularity, the time-consuming traffic collection in *TA* architectures is replaced by a fixed schedule of pre-determined topologies that maintain high connectivity regardless of traffic. Routing must now account for different topologies across time slices, introducing new challenges like per-time-slice routing and discontinuous paths, where packets may wait at intermediate hops for circuit availability. These requirements go beyond the capabilities of the traditional SDN paradigm.

We propose the *time-flow table* abstraction to address the new routing needs of *TO* architectures and remain backward compatible to *TA* ones. We define *arrival time slice* in the table to match incoming packets to different routing behaviors based on their entry time at the ToR, and define *departure time slice* to allow packets to exit at a scheduled time, aligning with circuit availability. When both arrival and departure time slices are set as wildcards, the time-flow table functions as a standard flow table, suitable for *TA* architectures. As we will show in §4, this abstraction is expressive enough to present

all known routing schemes in both *TA* and *TO* architectures.

We provide API functions (§5) that enable users to realize various optical architectures with customized topologies and routing strategies using a simple Python script, eliminating the need to manage low-level optical circuits or program time-flow table entries. Lighthouse acts as the backend system to support the time-flow table, which is non-trivial work.

To put things in context, most *TO* architectures, particularly those use nanosecond-reconfigured OCSes for sub-microsecond time slices, have not been implemented. While studies have shown their hardware feasibility [10, 11] and theoretical capacities [6, 7, 42], system-level overheads are often overlooked, and their fine time scales are expected to challenge commodity network devices. Moreover, the development of RotorNet, the only fully implemented *TO* architecture, spanned seven years, from the initial hardware prototype [31] to a complete system [30]. Despite the extensive engineering efforts, RotorNet only supports time slices in the hundreds of microseconds and is not openly accessible to users.

In Lighthouse, we advance the state of the art in *TO* architectures by streamlining their implementation and offering easy user access. We explore the limit of commodity network devices in supporting *TO* architectures, such as the minimum achievable time slice duration. As a general framework, Lighthouse also supports *TA* architectures, incorporating them into the user API and backend system to replicate the already implemented or even deployed *TA* architectures.

To deliver a high-performance system, we build Lighthouse’ ToR system (§6) on programmable switches, leveraging their programmability to implement the time-flow table and their nanosecond-precision packet processing to support short time slices; and we build the host system (§7) using the `libvma` userspace library for low latency and transparency to TCP/UDP applications. We address a series of engineering challenges unique to optical DCNs, such as precise enforcement of time slices, packet buffering and scheduling for time-based departures, preventing packets from missing their scheduled departure under competing flows, keeping low ToR buffer usage under high traffic, and reusing software components for different workflows of *TA* and *TO* architectures.

Lighthouse benefits a diverse range of users:

- **Optics researchers** can plug in OCSes into Lighthouse to have a workable architecture, testing if their designed hardware delivers expected system-level performance.
- **System researchers** can implement various architectural and routing solutions, compare them side-by-side, and explore new protocols on top, like congestion control. If actual OCSes are unavailable, Lighthouse provides emulation of OCSes but with real switch and host stacks.
- **Network architects** can select suitable OCS devices for a targeted architecture by emulating their physical properties in Lighthouse. They can also validate correctness of an optical architecture before real-world deployment.
- **Students** can study optical DCNs using our Mininet

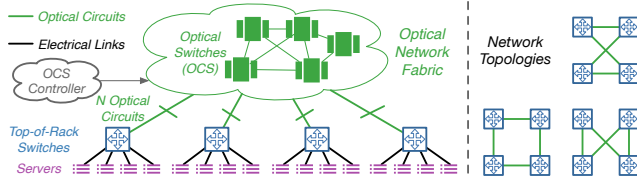


Figure 1: An example optical DCN and its 3 ToR-level topologies connected by different optical circuits over the OCSes.

education toolkit with Lighthouse, running Lighthouse in a virtual network without physical hardware.

We demonstrate generality of Lighthouse by implementing six *TA* and *TO* architectures and seven routing schemes on a testbed with both real and emulated OCSes, running cloud applications. It achieves minimum time slices of 2  $\mu$ s—the lowest time slice duration supported by commodity switches known to date. In a 108-ToR setting with production DCN traces, all system components function efficiently and Lighthouse keeps the usage of ToR buffer and other hardware resources under 13.8%. We also show how to build an example optical architecture with the user API and provide case studies of potential research problems that Lighthouse enables. We plan to open-source Lighthouse after the paper acceptance and foster a community for further research.

[This work does not raise any ethical issues.]

## 2 Background

In this section, we briefly introduce optical DCNs and their routing strategies to ease understanding of Lighthouse.

### 2.1 Optical DCNs

As illustrated in Fig. 1, an optical DCN has an *optical network fabric* in the core, formed by some internal structures of OCSes depending on the particular optical DCN architecture adopted. OCSes transmit optical signals in the *physical layer*, acting as waveguides like optical fibers but with the additional capability of circuit reconfiguration. An *optical controller*, e.g., a server or FPGA board, connects to the OCSes to establish *optical circuits* between communication endpoints, where a pair of endpoints has exclusive use of the circuit. The controller reconfigures these circuits to create different network topologies, such as the three topologies shown in Fig. 1.

As waveguides, OCSes are bufferless and unable to store or process packets, requiring the communication endpoints—electrical components immediately interconnected by the optical network fabric—to be coordinated to send packets only when the optical circuits are available. These endpoints are usually ToRs to aggregate traffic and save OCS ports [12–14, 16, 17, 28, 29, 31, 34, 35, 40, 43–45], as shown in Fig. 1, though they can also be end hosts or even accelerators in some proposals [10, 19, 30, 41]. In Lighthouse, we adhere to the mainstream architectures with optically interconnected ToRs.

Traffic-aware (*TA*) and traffic-oblivious (*TO*) are two types of optical DCNs reconfigured in different ways.

***TA* optical DCNs.** This design aims to establish circuits

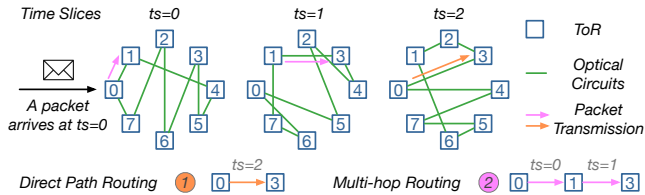


Figure 2: A routing example in a *TO* optical DCN. The arrows represent the paths for a packet from *ToR*<sub>1</sub> to *ToR*<sub>3</sub> arriving at time slice 0 under different routing schemes.

where heavy “elephant” flows occur, accommodating DCN traffic on demand. However, the control loop of traffic collection and topology computation takes milliseconds to seconds, delaying latency-sensitive “mice” flows as they wait for circuits to be ready. One solution (*TA-1*) uses a static network for mice flows, while sending elephant flows opportunistically over the optical circuits. The static network can either be a parallel electrical DCN, creating a so called electrical-optical hybrid DCN [16, 26, 40], or a default topology with some stable circuits [14, 17]. Another solution (*TA-2*) ensures every reconfigured topology is a connected graph, treating the optical DCN as a static network with occasional topology updates adapting to long-term traffic patterns [12, 13, 45]. Google’s Jupiter and Lightwave fabrics follow this approach, with reconfiguration intervals of minutes to hours [27, 35].

***TO* optical DCNs.** Unlike *TA* architectures that use optical circuits to boost elephant flow throughput, *TO* designs leverage advanced OCS technologies for rapid circuit reconfiguration, optimizing latency for mice flows [6, 7, 10, 29, 31, 42]. Each OCS configuration is held for a brief *time slice*, typically lasting only microseconds or even sub-microseconds, with a fixed *optical schedule* rotating through predefined topologies throughout time slices. These topologies maximize connectivity regardless of traffic patterns, often using expander graphs. The optical schedule repeats, each *optical cycle* having tens of time slices to fully diversify network connectivity over time.

## 2.2 Routing in Optical DCNs

Routing in most *TA* architectures is similar to that in static networks, as they treat each reconfigured topology independently, which is already supported by flow tables of the SDN paradigm. In *TA-1* architectures, mice flows are routed on the static topology, while elephant flows switch between the static topology and sporadic optical circuits. The flow table presents a default static route, and when a circuit becomes available, the optical controller updates it with a higher-priority route. *TA-2* architectures route traffic within each topology instance until it gets reconfigured, at which point the optical controller updates the flow table to shift traffic to the new paths.

Routing in *TO* architectures is more challenging due to the ultrashort time slices, where a packet in transit may cross multiple time slices, passing through different topologies. This requires routing paths to be pre-computed offline, based on the fixed optical schedule, and *ToR*s must execute the routing plan accurately for each time slice.

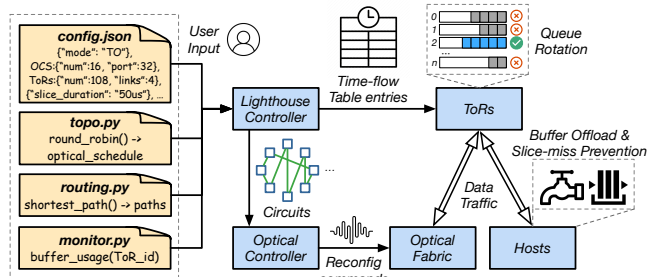


Figure 3: The workflow of Lighthouse.

As the example in Fig. 2 illustrates, a packet arriving at *ToR*<sub>0</sub> at time slice  $ts = 0$  and destined to *ToR*<sub>3</sub> can either wait until  $ts = 2$  to take the *direct* path ① when circuit *ToR*<sub>0</sub> ↔ *ToR*<sub>3</sub> appears, or can go through a more readily available *multi-hop* path ② via the intermediate hop *ToR*<sub>1</sub>. Multi-hop paths can happen in the same time slice [29] or across time slices [10, 23, 24, 31]. In this example, path ② crosses two time slices: the packet reaches *ToR*<sub>1</sub> in  $ts = 0$  over circuit *ToR*<sub>0</sub> ↔ *ToR*<sub>1</sub>, then waits until  $ts = 1$  for circuit *ToR*<sub>1</sub> ↔ *ToR*<sub>3</sub> to become available.

This time-based routing is fundamentally different from that of static networks, posing two additional requirements:

*Req 1:* To determine the time slice in which a packet arrives and map it to the corresponding routing path.

*Req 2:* To buffer the packet if it needs to be sent in a different time slice than the one in which it arrives.

As a general framework, Lighthouse must fulfill these new requirements of *TO* architectures, while being compatible with the traditional SDN paradigm used by *TA* architectures.

## 3 System Overview

Lighthouse addresses the additional routing challenges inherent in *TO* architectures (§2) while also supporting *TA* architectures (§8). In this section, we provide an overview of Lighthouse, focusing on the more complex *TO* architectures. Support for *TA* architectures is explained in §8.

We adopt a *ToR-centric design* for Lighthouse using programmable switches, with hosts supplementing the system performance. This design is based on two main considerations: (1) as explained in §2.1, *ToR*s serve as direct access points to the optical network fabric and are easier to scale up than hosts, and (2) the nanosecond-scale packet processing and transmission capabilities of programmable switches better match the fine time slices in *TO* architectures, allowing us to determine the minimum achievable time slice duration.

*ToR*s need to be synchronized with the optical controller accurately in *TO* architectures to stay aligned with the optical schedule. We have achieved nanosecond-precision synchronization in a separate work [22].

Our key solution in Lighthouse is the *time-flow table* abstraction (§4). Compared to the traditional flow table, it highlights *the notion of time* to meet the requirements of time-based routing in *TO* architectures (§2.2). As shown in Fig. 4, for *Req 1* in §2.2, we define *arrival time slice* as a *match field*,

ToR 0				ToR 0				ToR 1				ToR 0				ToR 0			
Arrival Slice	Dst.	Egress Port	Departure Slice	Arrival Slice	Dst.	Egress Port	Departure Slice	Arrival Slice	Dst.	Egress Port	Departure Slice	Arrival Slice	Dst.	Egress Port	Departure Slice	Arrival Slice	Dst.	Source Routing Action	
0	3	2	2	0	3	1	0	0	3	2	1	*	3	2	*	0	3	Hops:<Egress Port, Departure Slice>	
(a) Direct path				(b) Multi-hop path				(c) Static Topology				(d) Multi-hop Source Routing							
																		<1,0>,<2,1>	

Figure 4: Time-flow table examples for: (a) direct path ① and (b) multi-hop path ② in Fig. 2, (c) a static path in a TA architecture or traditional DCN, and (d) source routing realization of path ②, i.e., equivalent of per-hop lookup in (b).

allowing a ToR to determine the time slice of a packet upon arrival and map it to the appropriate path; for *Req 2*, we define *departure time slice* as an *action field* to enable routing protocols that may dispatch packets in future time slices [23, 24, 31]. The time-flow table is backward-compatible with regular flow tables, by setting arrival and departure time slices as wildcards, thereby supporting TA architectures as well.

The entire Lighthouse system is designed to facilitate the time-flow table abstraction. We provide user API functions (§5) to avoid requiring users to manually program the low-level time-flow table entries and optical circuits. As the system workflow shows in Fig. 3, users first supply a configuration file (`config.json`) specifying the basic DCN setup, including the TA/TO mode, the number and port counts of OCSes, their connected structure, reconfiguration delay, time slice duration, the number of ToRs, their connections and bandwidth to the OCSes, and the number of hosts per ToR. Users then write Python scripts for topology (`topo.py`), routing (`routing.py`), and monitoring (`monitor.py`) using the API functions listed in Table 1. We show an example in §9.1.

Lighthouse uses a centralized controller, co-located with or directly connected to the optical controller, to handle user inputs. The parameters in `config.json` must match the physical network setup. Before bringing the network online, the Lighthouse controller performs sanity checks, such as ping tests, to verify connectivity. The `topo.py` script defines the topology for each time slice, which the Lighthouse controller compiles into an optical schedule specifying the circuits per OCS for each time slice. After verifying that the schedule is feasible with the physical network setup, the Lighthouse controller loads it onto the optical controller.

The `routing.py` script provides routing paths for each source-destination ToR pair per time slice, which the Lighthouse controller translates into time-flow table entries for each ToR. For per-hop lookups [24, 31], paths are decomposed into next-hop ToRs, while for source routing [23, 29], entries are generated at the source ToR embedding the entire path. Since the Lighthouse controller connects to the ToRs via the optical network fabric, it first instructs the optical controller to configure the OCSes into a connected graph to load the time-flow table entries onto the ToRs. It also communicates the periodic monitoring needs in `monitor.py` to the ToRs, such as buffer usage and throughput metrics.

After the preparations are complete, the optical controller self-regulates the time slices using its internal clock and sends reconfiguration commands to the OCSes to execute the optical schedule. The ToRs, synchronized with the optical controller already, are also aware of the start of each time slice.

Realizing the time-flow table involves buffering packets until their scheduled departure time slices. While traditionally deemed impossible, we achieve this using the *queue pausing* feature of modern programmable switches, which allows for controlled pausing and resuming of queues [21]. For each egress port, we assign physical queues to specific time slices and buffer packets accordingly. All future queues are paused, keeping only the current time slice queue active. At the start of each time slice, *queue rotation* (§6) is triggered: the next time slice queue resumes while the current one pauses. We use circular queues to reduce the total number of queues needed.

Hosts complement the ToR-centric system with optional features to optimize performance. To prevent elephant flows from overwhelming the limited ToR buffer, we implement *flow pausing* on hosts, buffering elephant flows until direct circuits are available. For long time slices that strain ToR buffers, packets are offloaded to connected hosts.

Packets may miss their scheduled departure time slice because each circuit’s time slice can send a fixed amount of data. If flows from multiple sources sharing the circuit exceed this limit, some packets will not fit within the time slice. We implement *admission control* on ToRs: when the data limit is reached, traffic push-back is triggered and a notification is sent to the source host, which then uses flow pausing to halt packets to the ToR for the rest of the time slice. Our host system (§7) utilizes the `libvma` userspace library to achieve low latency and maintain transparency for TCP/UDP applications.

## 4 Time-Flow Table

We introduced the time-flow table in §3. In this section, we use examples from Fig. 4 to demonstrate its expressiveness in representing diverse routing schemes in TA and TO optical DCNs, specifically with routing paths ① and ② from Fig. 2.

**Direct-path routing.** Fig. 4 (a) shows the time-flow table of *ToR<sub>0</sub>* for the direct path ① from *ToR<sub>0</sub>* to *ToR<sub>3</sub>*. A packet arriving at time slice  $ts = 0$  must wait until  $ts = 2$  for the direct circuit *ToR<sub>0</sub>* ↔ *ToR<sub>3</sub>*, so the arrival time slice is set to 0, and the departure time slice is set to 2.

**Multi-hop routing.** For the multi-hop path ② via *ToR<sub>1</sub>*, the packet is forwarded immediately from *ToR<sub>0</sub>* to *ToR<sub>1</sub>* at  $ts = 0$ , so both the arrival and departure time slices in *ToR<sub>0</sub>*’s time-flow table in Fig. 4 (b) are set to 0. At *ToR<sub>1</sub>*, the packet arrives at  $ts = 0$  (through circuit *ToR<sub>0</sub>* ↔ *ToR<sub>1</sub>*) and waits until  $ts = 1$  to be sent to *ToR<sub>3</sub>*, so *ToR<sub>1</sub>*’s time-flow table has an arrival time slice of 0 and a departure time slice of 1.

**Routing in TA architectures.** The time-flow table reduces to a standard flow table if both the arrival and departure time slices are set to wildcards, as shown in Fig. 4 (c), allowing

Table 1: User API functions for *TO* architectures, those for *TA* architectures are in Appx. Table 5.

Category	APIs	Description
Topology	<code>connect(ToR1, port1, ToR2, port2, ts) → bool</code>	Primitive function connecting <code>port1</code> of <code>ToR1</code> to <code>port2</code> of <code>ToR2</code> in times slice <code>ts</code> .
	<code>topo() → bool</code> ↳ <code>round_robin()</code> , <code>topo_opera()</code> , <code>topo_shale()</code>	Abstract function to generate an optical schedule with connections across time slices. Topology implementations materializing <code>topo()</code> using <code>connect()</code> as a building block.
Routing	<code>routing() → [path(src, dst, ts)]</code> ↳ <code>direct()</code> , <code>vlb()</code> , <code>opera()</code> , <code>ucmp()</code> , <code>hoho()</code>	Abstract function to generate paths from <code>src</code> ToR to <code>dst</code> ToR in <code>ts</code> . Routing implementations materializing <code>routing()</code> .
	<code>neighbors(ToR, ts) → [ToRs]</code>	Helper function returning all ToRs having direct circuits to ToR in <code>ts</code> .
	<code>earliest_path(src, dst, ts, max_hop) → [path]</code> <code>entries([path], LOOKUP, MULTIPATH) → null</code>	Helper function returning paths from <code>src</code> to <code>dst</code> most recent to <code>ts</code> within <code>max_hop</code> . Translate paths into ToR entries with source/hop lookup and packet/flow multi-pathing.
Monitoring	<code>buffer_usage(ToR, port, interval) → unsigned</code>	Query the buffer usage of <code>port</code> at ToR every <code>interval</code> .
	<code>bw_usage(ToR, port, interval) → unsigned</code>	Query the bandwidth usage of <code>port</code> at ToR every <code>interval</code> .

packets to be forwarded immediately upon arrival. As noted in §2.1, routing in *TA* architectures occurs in separate topology instances with static paths, which can be represented using flow tables. As the time-flow table reduces to a flow table, it supports *TA* architectures, as well as static DCNs.

**Source routing.** We have shown examples of per-hop routing lookup so far. Some routing schemes, however, cannot break down the paths into per-hop lookups and have to be implemented with source routing [23, 29]. Our time-flow table supports source routing by including the entire path in the action field at the source ToR, as a sequence of `<egress port, departure time slice>` tuples for each hop. For example, Fig. 4(d) is the source routing equivalent of the per-hop tables in Fig. 4(b), where the hops `<1,0>` and `<2,1>` for `ToR0` followed by `ToR1` are to be written to the packet.

**Multi-path routing.** Time-flow table supports both per-packet and per-flow multi-path routing, as required by certain solutions [6, 10, 23, 31], through an optional path hashing field. For example, per-packet hashing can be based on times-tamping or on the on-chip random number generator, while per-flow hashing using the five-tuple.

Future routing solutions will likely combine these mechanisms and can hence also be supported by time-flow table.

## 5 User API

Table 1 lists the topology, routing, and monitoring APIs for *TO* architectures, and the extra ones for *TA* architectures are explained in §8. We show how to use them in §9.1.

**Topology APIs.** We define the primitive function `connect()` to offer users full flexibility in programming optical connectivity. This function establishes a connection between two ToRs, `ToR1` and `ToR2`, through their optical uplink ports, `port1` and `port2`, in a given time slice `ts`. It serves as a building block for higher-level topology schedules.

The abstract function `topo()` enables creation of diverse topologies. We materialize it to implement topology schedules for *TO* architectures, such as the round-robin schedule in RotorNet [31] and Sirius [10], and round-robin variants in Opera [29] and Shale [6]. They call `connect()` to achieve the desired connection patterns. Users can also define custom topologies following the `topo()` signature.

Lighthouse compiles the schedule into detailed circuits for the OCSes based on the physical OCS structure specified in `config.json` and returns the verification result. If the

circuits are feasible, Lighthouse directs the optical controller to configure the circuits for the specified time slices.

**Routing APIs.** Similar to `topo()`, we define an abstract function `routing()` to embody the wide variety of routing algorithms. Recall from §2.2 that in *TO* architectures, there are different paths from a source ToR to a destination ToR depending on the arrival time slice of a prospective packet, thus `routing()` returns the full set of paths for every source-destination ToR pair per time slice. We materialize `routing()` for existing routing algorithms, including direct-path routing [31], VLB [10, 31], Opera [29], UCMP [23], and HOHO [24], and allow users to implement customized routing algorithms following the signature format.

We provide helper functions to simplify the implementation of specific routing algorithms. For example, `neighbors()` retrieves connected neighbors for a ToR in a time slice, useful for VLB, and `earliest_path()` finds the first path between a source ToR and a destination ToR since a given time slice, facilitating direct-path routing, UCMP, and HOHO. Finally, the paths are passed to `entries()` to be translated into time-flow table entries for each ToR. The Lighthouse controller decomposes these paths into next-hop ToRs for per-hop lookup or retains the entire path for source routing.

**Monitoring APIs.** We also provide telemetry API functions for network monitoring, such as `buffer_usage()` and `bw_usage()` for querying the buffer and bandwidth usage of a ToR port. It is simple to extend to new functions as required.

## 6 ToR System

Now, we introduce key components of the ToR system, which are tailor-made for the unique challenges of *TO* architectures, including time-based packet buffering and scheduling, detection of slice misses, and efficient mitigation of the misses.

### 6.1 Queue Rotation

As outlined in §3, we leverage the queue pausing and resuming capabilities of Tofino2 to enqueue packets meant to be sent out in a later time slice into a designated queue. The queue remains paused until the corresponding time slice begins, after which it is resumed and kept active for one time slice before being paused again.

We implement the calendar queues framework [38] to realize this design. A calendar queue is associated with a “calendar day”, and packets can be enqueued at a “rank” for a

future calendar day. A *calendar day* is a *time slice* in our case. We create a set of calendar queues per egress port, assigning each time slice a queue sequentially until queue exhaustion to wrap around. The *rank* of an ingress packet is the difference between its *departure time slice* and the *arrival time slice*.

Queue pausing and resuming can be triggered by any ingress packet in the data plane. We control this process using the on-chip packet generator available in programmable switches [18], which reliably sends a packet into the ingress pipeline at a specified time interval. We configure this interval to match the *time slice duration*. Since the ToRs are synchronized with the optical controller (§3), the packet generator sends a packet at the start of each time slice to initiate *queue rotation* across all egress ports. This rotation pauses the currently active queue and resumes the queue for the upcoming time slice. Each ToR keeps track of the *active queue* for the current time slice, which is consistent across all egress ports.

Fig. 5 illustrates two sets of calendar queues at egress ports  $p=2$  and  $p=3$ . At time slice  $t_s=0$ , the active queue is  $q=0$  for all ports. An incoming packet matching the first entry in Fig. 5 (a) is mapped to  $q=0$  of  $p=2$  in Fig. 5 (b), because its departure time slice equals the arrival time slice, meaning it should be enqueued in the active queue for immediate transmission. When the time slice advances to  $t_s=1$ , queue rotation occurs, making  $q=1$  the active queue. Another packet arriving at this time matches the second entry and should be enqueued in  $q=2$  of  $p=3$ , to be sent out one time slice later as indicated by the difference between its departure and arrival time slices.

## 6.2 Slice-Miss Detection

As noted in §3, a packet may miss its scheduled departure time slice if competing flows overflow the circuit. To prevent this, packets enqueued in a calendar queue must fit within the remaining duration of that time slice. Otherwise, as the calendar queue is paused in the next time slice, extra packets would be queued for the entire optical cycle until the queue becomes active again, resulting in excessive queuing delays.

Detection of slice misses is challenging because accurate occupancy information for the calendar queue (an egress queue) is not available in the ingress pipeline before packet admission. Commercial switches lack this capability, and although Intel Tofino2’s “ghost thread” feature claims to provide it [21], our tests showed that queue occupancy readings are outdated by milliseconds. Other approaches, like informing queue occupancy through egress-to-ingress recirculation, introduce delays on the microsecond scale [46]. Both are impractical for the ultrashort time slices in *TO* architectures.

To address this issue, we implement a queue occupancy estimation method using a register array in the ingress pipeline to track each calendar queue’s occupancy. Ideally, these occupancy registers should be updated whenever packets are enqueued and dequeued. However, since registers at the ingress pipeline can only be updated by ingress packets, we increment the queue’s occupancy by the packet size upon enqueue-

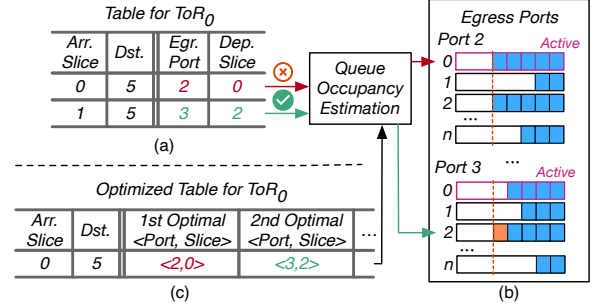


Figure 5: Example of packet processing on a ToR, assuming the active calendar queue is  $q=0$  for time slice  $t_s=0$ .

ing, while for dequeuing, we estimate occupancy reduction through periodic updates.

We use packet generator to create an ingress packet at every *update interval* to trigger updates. As dequeuing happens at line rate, the packet triggers the occupancy register of the active queue to decrease by the product of the *link bandwidth* and the *update interval*, or sets it to zero if the result is negative, indicating the queue has emptied. As shown in Fig. 12, an update interval of 50ns results in less than one packet estimation error at minimal pipeline processing overhead.

We make queue occupancy estimation a common module for slice-miss prevention in *TO* architectures. For example, Sirius and Shale query the occupancy of candidate intermediate ToRs to send packets to the least occupied ones [6, 10]; Opera caps queue occupancy and drops packets exceeding this limit [29]; UCMP and HOHO check queue occupancy to defer packets that cannot fit within the intended time slice to a later one [23, 24]. Besides supporting these mechanisms, as detailed in §7, we also use push-back messages to halt flows at their origin, preventing overwhelming the circuits.

## 6.3 Recirculation-Free Rerouting

Since *TO* architectures pre-compute routing paths offline (§2.2), it is often necessary to adjust these paths at runtime accounting for queuing information. For instance, if an incoming packet incurs slice miss (§6.2), rerouting it to a later time slice [23, 24] can achieve higher throughput and lower latency than dropping the packet [29]. Lighthouse thus supports this rerouting mechanism not only as required by existing routing proposals but also to benefit future designs.

Naïvely, existing routing solutions propose to recirculate the packet and re-match it to a later time slice with a different path, as if the packet arrived at a later time slice [23, 24]. As shown in Fig. 5 (a), a packet arriving at  $t_s=0$  initially intends to be enqueued in  $q=0$  of  $p=2$  based on the first entry of the time-flow table. However, queue occupancy estimation (§6.2) indicates that the queue is full, causing slice-miss detection to reject the packet. The packet is then recirculated and re-matched to the second entry, successfully passing slice-miss detection and being enqueued in  $q=2$  of  $p=3$ .

Recirculation costs extra pipeline processing and incurs a microsecond-scale delay, so we design a *one-shot lookup*

approach to avoid recirculation. The main challenge is that, due to the hardware restrictions of the programmable switch pipeline, the time-flow table (§4) and the queue occupancy register array (§6.2) can only be accessed once by each packet. This limitation necessitates packet recirculation to check queue availability for the next optimal path(s).

We solve this problem by caching the full/unfull state of each calendar queue into a bit array stored in a single register. To keep the bit array consistent with the queue occupancy register, whenever the occupancy register reaches the admission threshold, the corresponding bit in the bit array changes accordingly. Although a register permits only single access per packet, we can retrieve all queue states at once.

We optimize the time-flow table to align with this design. As shown in Fig. 5 (c), we combine the optimal path, e.g., the first entry in Fig. 5 (a), and the next best path(s) for subsequent time slices, e.g., the second entry in Fig. 5 (a), into a single lookup entry by concatenating their <egress port, departure time slice> tuples in the action field. This allows an ingress packet to evaluate all queues in a single access to the queue state bit array, selecting the most suitable path that is not full.

This hardware resource usage of this design is within the capacity of ToRs. Registers on Tofino2 switches support up to 128 bits, for 128 time slices, which is more than sufficient for *TO* architectures that usually have tens of time slices.

## 7 Host System

The host system provides optional features for the ToR-centric Lighthouse design for enhanced performance, complementing fine-grained packet processing at the ToRs. This section details the flow pausing functionality on hosts and its role in facilitating buffer offloading and traffic push-back from ToRs.

**Flow pausing.** While the general abstraction of time-flow table is expressive to support rich routing schemes (§4) and calendar queues (§6.1) provide buffering for all traffic, elephant flows place a substantial burden on ToR buffers. It is more efficient to route elephant flows over direct circuits, releasing packets from senders only when the circuits are available. To achieve this, we implement flow pausing on hosts to alleviate the exclusive burden of buffering from ToRs.

We utilize *flow aging* [9] to identify elephant flows without explicit flow size information. ToRs broadcast *signal messages* to the connected hosts, notifying them of upcoming circuit connections. We implement flow pausing with the user-space `libvma` library to achieve high performance and transparency to TCP/UDP applications [2]. `libvma` links sockets to the user-space `lwIP` stack, where we intercept socket send calls to suspend sending out data from the segment queue until the circuit is ready. Suspending and resuming applications require no additional memory buffers beyond the segment queue, as applications are naturally pushed back by the socket interface when the segment queue reaches its capacity. Fig. 9 demonstrates high throughput of our implementation.

**Buffer offloading.** As shown in Table 2, buffer memory

on ToRs is generally adequate for *TO* architectures, which operate with short time slices in the microsecond or even sub-microsecond range, and employ routing solutions designed to minimize latency. However, as a general framework, Lighthouse also accounts for worst-case scenarios involving longer time slices—potentially extending to several hundred microseconds—and routing schemes with relatively high latency, such as VLB where packets may need to wait for an entire optical cycle [31]. In such cases, Lighthouse offloads calendar queues to hosts to reduce buffer usage on ToRs.

Each ToR only keeps  $N$  calendar queues per egress port for the immediate future and stores the rest for later time slices onto hosts under it. As the time slices corresponding to the host-resident calendar queues approach, the packets are sent back to the ToR in advance, guided by circuit notification messages. To keep the logic on ToRs lightweight, they randomly select hosts to balance the load and delegate bookkeeping to hosts, which initiate returning of offloaded packets. We implement buffer offloading also with `libvma`. We dedicate an application per host to isolate it from the main data path and ensure low latency. The offloaded packets are stored similar to paused flows as described above.

**Traffic push-back.** As discussed in §6.2, *TO* architectures have proposed various remedies for slice misses, such as explicit drop notifications [29] and rerouting to future time slices [23, 24]. In Lighthouse, we complement them by implementing traffic push-back to solve the problem at its origin.

A packet incurring slice miss indicates that the designated calendar queue is full, and subsequent packets to this queue will also be rejected. If enabled, a rejected packet triggers a *push-back* message with the time slice of the full queue. The message is not sent to the sender host alone, but to the sender ToR, which then broadcasts it to all connected hosts, preventing them from sending to the destination ToR during that time slice using flow pausing. The broadcast increases the push-back coverage to hosts that may attempt to send to the same queue. The specific optical architecture can decide when to trigger push-back, such as upon packet drops [29] or after rerouting packets  $N$  times.

## 8 Support for *TA* Architectures

*TA* architectures follow a different workflow from Fig. 3, where topology updates are dynamic and traffic-driven, not based on a pre-determined optical schedule. As the extra APIs in Appx. Table 5 show, instead of specifying connections, the topology API provides a scheduling algorithm that computes circuit connections from the ToR-level traffic matrix. We have implemented BvN [39], hotspot scheduling [34], and multi-level factorization [35] algorithms for the *c-Through*, *Mordia*, and *Jupiter* architectures. After computing, circuit connections are enforced using `connect()` from Table 1. Since *TA* architectures use topology update intervals instead of time slices, users specify the interval in `config.json` and set `ts = -1` when reusing APIs from *TO* architectures. The routing API

```

1 net = LighthouseNet(config)
2 assert net.round_robin() == True,
3     "Invalid Topology."
4 paths = net.direct()
5 entries(paths, lookup=HOP,
6     multipath=None)
7 #Monitor
8 for tor in config.tors:
9     for port in tor.ports:
10        dashboard.update(
11            buffer_usage(tor, port, "1ms"))
12
13 def round_robin(self) -> bool:
14     tor_num = self.config.tor_num
15     assert tor_num % 2 == 0
16     tors = list(range(tor_num))
17     for ts in range(tor_num-1):
18         for i in range(tor_num // 2):
19             if not self.connect(tors[i], 0,
20                 tors[-i-1], 0, ts):
21                 return False
22         tors.insert(1, tors.pop(-1))
23         return True
24
25 def direct(self) -> paths:
26     tor_num = self.config.tor_num
27     paths = []
28     for ts in range(ts_num):
29         for src in range(tor_num):
30             for dst in range(tor_num):
31                 if src != dst:
32                     paths.append(
33                         self.earliest_path(
34                             src, dst, max_hop=1))
35     return paths

```

(a) Steps to set up an optical DCN. (b) Realizing round-robin topology. (c) Realizing direct-path routing.

Figure 6: Code snippets of implementing a basic optical architecture using the Lighthouse APIs.

uses static network routing algorithms, as each topology remains static between reconfigurations. To support c-Through, Mordia, and Jupiter, we have implemented ECMP,  $k$ -shortest path, and reused `direct()` from *TO* architectures.

We reuse *TO* software components to support *TA* needs. Queue occupancy estimation (§6.2) is exposed as an RPC service on the ToR control plane, enabling Lighthouse to query ToRs for the traffic matrix. For direct-path routing of elephant flows in *TA* architectures, we reuse the flow-pausing feature (§7) for host-side packet buffering. The time-flow table (§4) defaults to a standard flow table by wildcarding the arrival and departure time slices, and the calendar queues (§6.1) revert to regular queues when queue rotation is disabled.

## 9 Evaluation

In this section, we showcase the capabilities of Lighthouse as a general framework and evaluate its system performance. We begin by demonstrating how to use the user API (§5) to construct a basic optical architecture (§9.1), followed by examples of potential research questions that Lighthouse enables us to explore (§9.2). Finally, we present benchmarking studies to assess the system’s performance at scale (§9.3).

### 9.1 How to use Lighthouse?

Lighthouse lowers the barrier to entry for systems research in optical networking by greatly simplifying the implementation of optical architectures through its user-friendly API (Table 1). As the code snippets show in Fig. 6, researchers can define an optical architecture using a straightforward Python script that calls the API functions, while Lighthouse handles all backend interactions with the optical fabric.

Fig. 6a presents the main logic. A user can easily create an optical architecture by instantiating an `LighthouseNet` object, which reads in the system configuration `config.json`. The user can then set up a round-robin topology and generate direct-path routing by invoking the topology and routing APIs `round_robin()` and `direct()`, respectively. The program proceeds only if the topology is valid, meaning the ToR connections form legitimate circuits within the OCSes. The `entries()` function converts paths into time-flow table entries, configured for per-hop lookup and without multi-pathing. The monitoring API `buffer_usage()` can be called to report buffer usage for each ToR port every 1 ms.

The implementation of `round_robin()` and `direct()` is



(a) Testbed photo. (b) Testbed diagram.

Figure 7: Testbed setup (servers in 7a are omitted from 7b).

detailed in Fig. 6b and 6c. For simplicity, we demonstrate a basic round-robin topology in Fig. 6b with one optical port per ToR, using the circle method [20]. This method adds all ToRs to a list (line 15) and connects them in pairs (lines 18-19). The list is reordered in each time slice to permute connections (line 21). The library function `connect()` establishes connections between port 0 of every two ToRs, converting them into optical circuits based on the OCS structure in `config.json` and returning the sanity check result of the circuits (line 20). The topology is valid if all connections succeed (line 22). On the other hand, Fig. 6c shows direct-path routing using the helper function `earliest_path()` with `max_hop` set to 1, which generates direct (one-hop) paths from all source ToRs to all destination ToRs across all time slices (lines 30-32).

As described in §3, the code runs on the Lighthouse controller, which directs the optical controller to set up the circuits and loads the generated time-flow table entries to the ToRs. The optical DCN is ready to carry traffic afterwards. Additionally, the system dashboard on the Lighthouse controller visualizes the topologies across different time slices and displays network status based on monitoring data.

### 9.2 What research does Lighthouse support?

Lighthouse enables systems research by abstracting the complexities of optical hardware, allowing researchers to explore high-level questions without deep domain knowledge about optics. Below, we show three of many possible use cases of Lighthouse as a framework for systems research.

**Testbed.** To demonstrate the full capabilities of Lighthouse, we build a testbed with both real and emulated optical fabrics, as well as a traditional electrical fabric. As shown in Fig. 7, the setup includes a Polatis Series 6000 MEMS OCS, four EdgeCore DCS810 Intel Tofino2 switches, and four servers equipped with Mellanox ConnectX-5 100 Gbps dual-port NICs. The MEMS OCS functions as an optical network fabric. Two Tofino2 switches are each divided into



four logical ToRs (Fig. 7b), while the third Tofino2 switch emulates another optical fabric with flexible structures of emulated OCSes, and the fourth serves as an electrical fabric. Each of the eight ToRs connects to the OCS and the electrical fabric with a 400 Gbps link and to the emulated optical fabric with four 100 Gbps links to support flexible emulation. The servers’ dual-port NICs provide eight 100 Gbps links, each connected to a ToR to work as eight individual hosts.

**Traffic.** We run both latency-sensitive and throughput-intensive applications on the testbed to examine mice and elephant flows. We use the *Memcached* [3] key-value storage for the latency-sensitive application, running one Memcached server and seven Memslap [4] benchmarking clients each on a host. The clients perform SET operations at milliseconds intervals, writing 4.2 KB of data to the server. As for the throughput-intensive application, we run *ring allreduce* on the hosts using the *Gloo* collective communication library [1], with varying data sizes from 800 KB to 20 MB.

**Case I: realistic comparison of architectures.** Optical architectures are each a closed ecosystem and many have not been implemented end-to-end, making reproduction and performance comparison difficult unless in simulations. As shown later in §9.3, Lighthouse can support a wide range of optical architectures with a minimum time slice of 2  $\mu$ s, using real switch and host stacks. In this case study, we implement representative optical architectures and perform side-by-side comparison of them, including *c-Through* [40], *Jupiter* [35], and *Mordia* [34] from the *TA* class, and *RotorNet* [31] and *Opera* [29] from the *TO* class. We also include the traditional *Clos* [5] network for baseline comparison.

*Clos* relies on the electrical network fabric (Fig. 7), while the MEMS OCS, with tens of milliseconds long reconfiguration delays, supports *Jupiter* and *c-Through*. As a hybrid architecture, *c-Through* also connects to the electrical fabric, rate-limited to 10 Gbps for consistency with the original design. *Mordia*, *RotorNet*, and *Opera*, requiring finer-grained circuit reconfiguration, use the emulated optical fabric. We apply the native routing schemes and optical fabric settings for these architectures and also run *UCMP* [23] routing on top of *RotorNet* to show the latest performance of *TO* architectures.

Fig. 8 plots flow completion times (FCTs) of mice and elephant flows in the Memcached and Gloo applications. In Fig. 8a, *c-Through* shows similar mice flow FCTs to *Clos*. As a hybrid architecture, it uses the optical fabric only for elephant flows, while sending mice flows over electrical network, which has minimal impact on their FCTs. *Jupiter* improves FCTs by offering an optimized topology with fewer hops tailored to the traffic. *Mordia*, also a *TA* architecture, establishes circuits on demand. This results in low FCTs for flows immediately having an available circuit, but a long tail otherwise.

*TO* architectures such as *RotorNet* and *Opera* are more sensitive to routing due to their traffic-agnostic topologies. *RotorNet* employs VLB, which introduces significant circuit-waiting delays by waiting at intermediate hops, resulting in

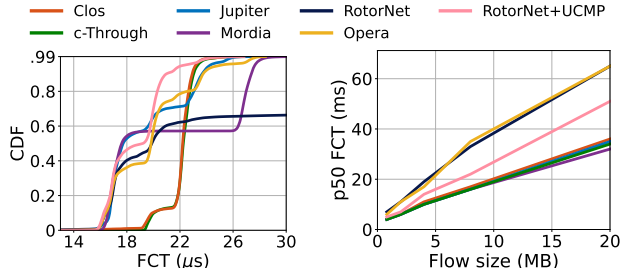


Figure 8: FCTs of (a) Memcached and (b) Gloo allreduce.

long tail FCT. In contrast, *Opera* has low FCTs utilizing longer but always-available paths. *UCMP* achieves even lower FCTs by further reducing path length.

For elephant flows in Fig. 8b, *TA* architectures *c-Through*, *Jupiter*, and *Mordia* exhibit similar FCTs as *Clos*. They establish a ring topology using optical circuits that matches the traffic perfectly. *TO* architectures *RotorNet* and *Opera*, however, double the FCTs as the circuits are available only half the time. *UCMP* improves throughput with more efficient routes, leading to reduced FCTs.

This case study confirms the design goals of different architectures and validates correctness of our Lighthouse implementation: *TA* architectures mostly optimize elephant flow throughput, while *TO* architectures focus on reducing mice flow latency, and the choice of architectures should consider the characteristics of the traffic workload. Researchers can follow this approach to reproduce and compare with former designs, as well as explore specific design aspects more deeply.

**Case II: investigation of the transport layer.** Optical DCN researchers are increasingly focused on transport performance due to the unique challenges posed by dynamic paths. For instance, TCP variants like reTCP [33] and TDTCP [15] were recently proposed for electrical-optical hybrid networks to handle the fluctuating bandwidth capacity, both evaluated on the Etalon emulator [33]. However, we argue that transport in general *TO* architectures is more challenging due to frequent path changes across multiple time slices, rather than just between two fabrics. A reason for the lack of research in this area is the absence of experimental platforms, as Etalon only supports hybrid architectures.

In this case study, we demonstrate how Lighthouse enables investigation into the transport layer over different *TO* solutions. We measure the throughput of long-lasting *iperf3* flows between hosts on *Clos*, *RotorNet* with VLB and direct-path routing, and finally a hybrid version of *RotorNet* with 100 Gbps bandwidth through the optical fabric and 10 Gbps bandwidth through the electrical fabric, as in TDTCP.

As shown in Fig. 9(a), the 40 Gbps throughput in *Clos* is the upper bound for *iperf3* on our testbed due to the CPU-bound. As expected, for direct-path routing our host system with flow pausing (§7) achieves roughly half that throughput due to the circuit being available 50% of the times. On the other hand, VLB exhibits abysmal throughput compared to the baseline. Surprisingly, also hybrid *RotorNet* lags behind direct-path

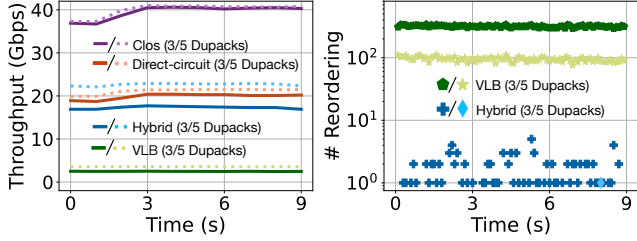


Figure 9: (a) TCP throughput and (b) number of packet reordering events with iperf traffic.

routing. We attribute this gap to the TCP performance under packet reordering, as measured in Fig. 9(b).

To further validate our observation, we increase the TCP dupack threshold from the default 3 to 5, which almost eliminates reordering events in hybrid RotorNet and pushes the throughput back to the expected value, i.e., near 25 Gbps with 50% of data through the electrical fabric and 50% of data through the optical fabric. While slightly improved, VLB throughput is still low due to excessive reordering.

We have demonstrated the troubleshooting process for transport performance in this case study. Similarly, researchers can tune transport protocol parameters and evaluate newly designed protocols for optical DCNs with Lighthouse.

**Case III: choice of optical hardware.** Numerous OCS designs have been developed by the optics community. These works focus on device-level characteristics like port count, reconfiguration delay, lossiness, and manufacturing costs, seldom extending to full optical architectures. Thus, network architects traditionally select devices based on a general understanding of trade-offs between these factors, without insight into how these attributes impact overall network performance.

In this case study, we demonstrate how Lighthouse facilitates more informed decisions on optical hardware selection through its emulation capabilities. We sample four recently proposed OCS technologies and emulate the RotorNet architecture with them by inputting their physical characteristics and OCS structures into the `config.json` file. Fig. 10 shows the FCTs for the Memcached application (as in Fig. 8a) relative to the supported time slice duration of each OCS device.

In Fig. 10a, RotorNet’s native VLB routing exhibits long tail FCTs proportional to the time slice duration, as packets are randomly routed through intermediate ToRs. In the worst case, a packet waits an entire optical cycle at the intermediate ToR for a direct circuit to the destination. This result suggests the shorter the time slice, the merrier, but OCS costs rise substantially with shorter time slices. Fortunately, Fig. 10b presents a different trade-off with UCMP routing, which strategically selects intermediate ToRs, reducing FCTs and making performance less sensitive to time slice duration. UCMP is less effective under very short time slices, like 2  $\mu$ s, due to higher risks of slice misses causing more packet rerouting. The best performance occurs at 100  $\mu$ s time slices, with little difference at 200  $\mu$ s, allowing good performance with more cost-effective OCS devices.

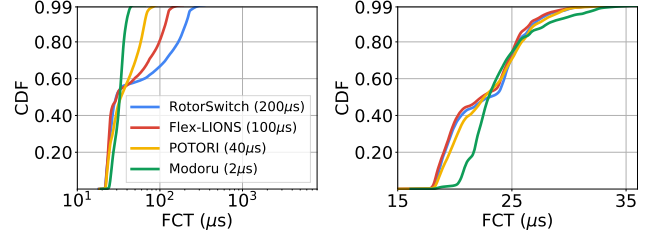


Figure 10: Mice flow FCTs on RotorNet with OCSes of different time slice durations, under (a) VLB and (b) UCMP routing.

We have shown a simple case of finding the performance-cost sweet spot for OCS devices based on a specific traffic workload. Lighthouse enables researchers and network architects to conduct more sophisticated emulations to explore the interplay between optical hardware properties, network architectures, routing strategies, and higher-layer protocols.

### 9.3 What is the system performance at scale?

After the case studies on a small testbed (§9.2), we further evaluate the performance of different system components to validate our design decisions. We reuse the testbed equipment (Fig. 7) to construct a setting at scale and run production DCN traces. Users of Lighthouse can follow the same approach for large-scale analytics with limited hardware availability.

**Experimental setup.** We emulate the 108-ToR topology from the Opera paper [29] because its rigid ToR and OCS structures make it compatible with other optical architectures. In Opera, each ToR has six 100 Gbps uplinks to the optical network fabric and six 100 Gbps downlinks to hosts. We implement a single representative ToR on a Tofino2 switch, referred to as the *observed ToR*, and connect it to another Tofino2 switch through six 100 Gbps links, which emulates the optical network fabric. We populate the full time-flow table on the observed ToR with entries for the 108-ToR network, and the emulated optical fabric operates at full network scale. Three servers with dual-port NICs are connected to the observed ToR, acting as six hosts with one 100 Gbps link each. We replay the widely-used RPC [32], Hadoop [36], and KV store [8] DCN traces on the hosts and scale the load to reach 40% core link utilization as in production DCNs [37].

**Queue rotation efficiency.** Rotation of calendar queues (§6.1) must be aligned precisely with the time slices, but delays between ToRs, including the switch pipeline processing, packet serialization, and on-wire propagation delays, interfere with the accuracy of time calculation. We measure these delays from the observed ToR back to itself through the MEMS OCS to use the same clock for accurate timestamping. This is done by continuously sending packets at line rate using the on-chip packet generator on the switch. The ToR-to-ToR delay is from when queue rotation is triggered on the sender side to when each packet arrives at the Rx MAC of the receiver side. Fig. 11 plots the delays with different packet sizes. The minimum delay is 1287 ns, which we can offset by starting queue rotation earlier to ensure that the least delayed

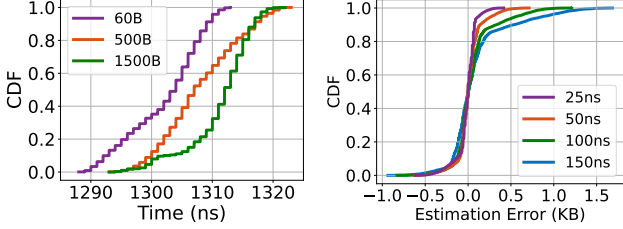


Figure 11: ToR-to-ToR delay with different packet sizes. Figure 12: Queue occupancy estimation error under different update intervals.

packet catches the upcoming circuit. The maximum delay is 1324 ns, indicating that the most delayed packet arrives  $1324 - 1287 = 34$  ns after the circuit is established. As will be discussed soon, no packet should be sent in this 34 ns to avoid packet loss, which only wastes  $34 \text{ ns} / 2 \mu\text{s} = 1.7\%$  of the 2  $\mu\text{s}$  minimum time slice duration.

**Queue occupancy estimation accuracy.** The error of queue occupancy estimation (§6.2) is the difference between our estimated queue occupancy from the ingress pipeline and the ground-truth queue occupancy read by an egress packet. We measure it with the above setting (in Fig. 11) but combine line-rate traffic and bursty traffic to fill and drain the queue periodically. As shown in Fig. 12, the estimation accuracy increases with the update interval. We find 50 ns draws a good balance between the estimation accuracy and the consumption of pipeline processing resources on the ToR. The estimation error is within 725 B, less than half MTU-size packet, and the packet generator sends one packet every 50 ns (or at 20 Mpps), which creates only 1.3% pipeline forward overhead on a Tofino2 switch with 1.5 Bpps processing capacity.

**Minimum time slice duration.** Packets are subject to losses during circuit reconfiguration, so most optical DCNs incorporate a guardband to block traffic during that period. In Lighthouse, we account for delays aside from the fixed circuit reconfiguration time, which is determined by the chosen optical hardware. The guardband duration is the larger between the two as they can overlap in time. The time slice duration is typically set to at least  $10\times$  the guardband duration to ensure a duty cycle of over 90%. The delays enable us to determine the minimum achievable time slice duration by Lighthouse as a general framework for diverse optical architectures.

As mentioned earlier, the 34 ns queue rotation variance (Fig. 11) should be covered by the guardband. The queue occupancy estimation error of 725 B (Fig. 12) should also be considered. It translates to 58 ns delay under 100 Gbps bandwidth, meaning packets may get impacted by false negatives for 58 ns, where a full queue is mistakenly seen as not full. In addition, our separate synchronization work demonstrates at most 28 ns sync errors for a 192-ToR optical DCN [22]. The guardband should, hence, should account for  $28 \times 2 = 56$  ns of potential sync errors either above or below the actual clock time. Therefore, the guardband is at least  $34 + 58 + 56 = 148$  ns. Adding some headroom for runtime variations, we set the

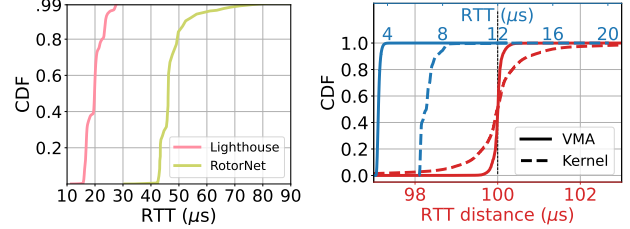


Figure 13: UDP latency in Lighthouse vs. in RotorNet (Fig.15 blue curve in [30]). Figure 14: RTT delay (blue) and RTT distance to the 100  $\mu\text{s}$  interval (red).

guardband to be 200 ns. Lighthouse can thus support a minimum time slice duration of  $200 \text{ ns} \times 10 = 2 \mu\text{s}$ , which is the shortest time slice duration to date implemented with commodity devices. We observe no packet loss in all the experiments with this guardband value.

**Emulation accuracy.** We have verified the correctness of our Lighthouse implementation in Fig. 8 on both real and emulated optical fabrics, showing that the performance of various optical architectures realized on top of Lighthouse aligns with their design goals. To further assess Lighthouse’ emulation accuracy, we reproduce experimental results from the “Realizing RotorNet” paper [30], which is the only end-to-end implemented *TO* architecture so far, with actual OCSes.

We replicate the UDP RTT latency experiment by continuously sending UDP packets from one host to another and measuring the RTT for each packet. Fig. 13 compares Lighthouse’ results on the emulated optical fabric with RotorNet’s on real OCSes. Both curves exhibit similar latency distribution patterns, with stepped RTT increases corresponding to additional routing hops. The similar curve shapes indicate comparable routing behaviors between our emulated fabric and the actual OCS fabric, confirming correctness of Lighthouse. Lighthouse achieves lower RTTs and eliminates the long tail because the ToR-centric implementation and `libvma` stack produce less delay and variance than RotorNet’s FPGA NICs and the kernel UDP implementation.

**Buffer usage.** VLB, HOHO, and UCMP are the only routing solutions that have packets wait at intermediate ToRs, so we evaluate ToR buffer usage with those. We run 300  $\mu\text{s}$  time slices, considered long for *TO* architectures. As shown in Table 2, HOHO and UCMP maintain low buffer usage across traces, as they prioritize latency by directing packets to the nearest time slices. In contrast, VLB causes packets to wait for extended periods at intermediate nodes. Nonetheless, the maximum buffer usage of 12.78 MB remains well below the 64 MB limit of Tofino2 switches, and buffer offloading to hosts (§7) reduces the buffer load to a minimal level. These results indicate that the calendar queues (§6.1) in our ToR system are sustainable for higher bandwidth in the future.

**Effectiveness of slice-miss prevention.** Among the routing schemes, HOHO is most vulnerable to slice-miss events, as it minimizes latency by always sending packets over the earliest available time slices, and is likely to overshoot. Hence, we evaluate our slice-miss prevention mechanisms, i.e., slice-

Table 2: 99.9%-ile buffer usage under different traces with 300  $\mu$ s slice duration. Total buffer on Tofino2 is 64 MB.

<i>Routings</i>	<i>VLB (offloaded)</i>	<i>HOHO</i>	<i>UCMP</i>
KV Store	9.48 MB (1.26 MB)	2.40 MB	2.44 MB
RPC	9.96 MB (1.38 MB)	3.06 MB	4.15 MB
Hadoop	12.78 MB (1.56 MB)	3.90 MB	6.54 MB

miss detection (§6.2) and traffic push back for mitigation (§7), specifically with HOHO.

We stress-test the calendar queues by increasing traffic load to 70% core link utilization, triggering our prevention mechanisms. As shown in Table 3, without slice-miss detection or push back (column 1), packets are always enqueued to the most desirable calendar queue, even when it exceeds the slice capacity. The queue pauses after the time slice ends, holding buffered packets until the next cycle(s), leading to long delays and packet loss. With slice-miss detection alone (column 2), loss rates and average delay decrease slightly as packets are deferred to later time slices when the primary queue is full, but queues eventually fill up, causing losses. When both mechanisms are combined (column 3), push back engages once the primary queue is full, and slice-miss detection handles in-flight traffic before senders react. This eliminates packet loss, and low queuing delay indicates most packets are enqueued in the primary calendar queue. These measures have similar effects on Opera and UCMP, reducing packet loss rate from 2.5% to 0% in Opera, also eliminating loss and reducing tail latency from 1.4 ms to 115  $\mu$ s in UCMP.

**Host system efficiency.** We have shown good performance of the host system (§7) in Fig. 9: flow pausing ensures expected throughput (50% of maximum throughput with 50% circuit availability) for direct-path routing without packet reordering. Here, we evaluate the stability of RTTs between ToRs and hosts, which is critical for buffer offloading.

We send 1500 B packets from the observed ToR to a connected host at 100  $\mu$ s intervals. The host returns them upon receipt to simulate offloading and retrieval. Fig. 14 shows our `libvma`-based implementation ensures stable RTTs: 95% of RTTs exhibit a small variance of 0.75  $\mu$ s, and their deviation from the expected 100  $\mu$ s intervals remains within  $\pm 0.25 \mu$ s. The performance is significantly better compared to a kernel module baseline, confirming the efficiency of `libvma`. In practice, we return offloaded packets to the ToR early to offset the base delay and variance. Packets arriving marginally earlier are buffered on the ToR consuming minimal memory.

**ToR resource usage.** As listed in Table 4, the resource usage of an Lighthouse-enabled ToR in the 108-ToR DCN is a small percentage. The low usage of SRAM, VLIW Actions, and TCAM indicates the efficient implementation of registers and lookup tables. Stateful ALU and Ternary Xbar have higher usage, due to the arithmetic calculations and branching operations for slice-miss detection. All the resources are under 13.8% of an Intel Tofino2 switch’s capacity, leaving sufficient room for Lighthouse to scale up to larger DCNs.

Table 3: Effectiveness of slice-miss prevention in HOHO with Hadoop/RPC/KV-store traces under 300  $\mu$ s time slices.

<i>Slice-Miss Detection</i>	$\times$	$\checkmark$	$\checkmark$
<i>Push Back</i>	$\times$	$\times$	$\checkmark$
Throughput (Gbps)	67/69/64	67/69/64	50/54/49
Loss Rate	1.1%/1.0%/2.1%	1.1%/1.0%/2.0%	0%/0%/0%
Average Delay	160/150/98 $\mu$ s	125/144/91 $\mu$ s	6/5/8 $\mu$ s
95%-ile Delay	2.2/2.2/2.1 ms	2.1/2.2/1.9 ms	85/90/83 $\mu$ s

Table 4: Hardware resource usage of Lighthouse on Tofino2.

<i>Resource</i>	<i>Usage</i>	<i>Resource</i>	<i>Usage</i>
SRAM	3.8%	TCAM	2.3%
Stateful ALU	9.4%	Ternary Xbar	13.8%
VLIW Actions	5.6%	Exact Xbar	7.8%

## 10 Related Work

In §2, we gave an overview of DCN architectures [6, 10, 12–14, 16, 17, 19, 25, 28, 29, 31, 34, 35, 40, 41, 43–45], and implemented six of them over the 2  $\mu$ s minimum time slice duration (§9.2), showing generality of Lighthouse. Our time-flow table abstraction applies to all architectures, regardless of constraints from today’s commodity devices, making it promising in realizing more architectures as technologies advance.

UCMP [23] and HOHO [24] are general routing algorithms for TO architectures. We realized them on Lighthouse and found out UCMP could reduce RotorNet’s performance sensitivity to optical hardware, potentially allowing for the use of more cost-effective OCSes (§9.2). Recent transport proposals of reTCP [33] and TDTCP [15] highlight the need for system designs atop of optical architectures, which validates the design purpose of Lighthouse. Our TCP throughput case study (§9.2) confirms packet reordering addressed in these works.

Closest to Lighthouse as an end-to-end testing platform is the Etalon emulator [33]. Lighthouse is more general and realistic. It supports all types of optical DCNs while Etalon is built for hybrid architectures only. Lighthouse can connect ToRs to real OCSes, while Etalon emulates the network fabric in a Click software switch. Lighthouse has the full switch and host implementations, while Etalon misses the switch stack and ties the hosts to the Docker virtualized environment.

## 11 Conclusion

This paper presents the design and realization of Lighthouse, an open research framework that promotes system innovation for optical DCNs. The fact that Lighthouse decouples software solutions from optical architectures will redefine the landscape of system research for optical DCNs. Since Lighthouse has abstracted out the complexity of optical hardware with the time-flow table, network and system researchers who lack domain knowledge on optical hardware can now contribute to optical DCNs by solving generic system problems. We envision classic topics such as routing, load balancing, and congestion control to burgeon for optical DCNs. Moving forward, we plan to test Lighthouse further with higher-speed OCSes and build a community of researchers and developers for optical DCNs after open-sourcing the code.

## References

- [1] Gloo. <https://github.com/facebookincubator/gloo>.
- [2] Mellanox Messaging Accelerator. <https://github.com/Mellanox/libvma/blob/master/README>.
- [3] Memcached. <https://memcached.org/>.
- [4] Memslap. <http://docs.libmemcached.org/bin/memslap.html>.
- [5] Mohammad Al-Fares, Alexander Loukissas, and Amin Vahdat. A scalable, commodity data center network architecture. *ACM SIGCOMM computer communication review*, 38(4):63–74, 2008.
- [6] Daniel Amir, Nitika Saran, Tegan Wilson, Robert Kleinberg, Vishal Shrivastav, and Hakim Weatherspoon. Shale: A practical, scalable oblivious reconfigurable network. In *Proceedings of the ACM SIGCOMM 2024 Conference*, pages 449–464, 2024.
- [7] Daniel Amir, Tegan Wilson, Vishal Shrivastav, Hakim Weatherspoon, Robert Kleinberg, and Rachit Agarwal. Optimal oblivious reconfigurable networks. In *Proceedings of the 54th Annual ACM SIGACT Symposium on Theory of Computing*, pages 1339–1352, 2022.
- [8] Berk Atikoglu, Yuehai Xu, Eitan Frachtenberg, Song Jiang, and Mike Paleczny. Workload analysis of a large-scale key-value store. In *Proceedings of the 12th ACM SIGMETRICS/PERFORMANCE joint international conference on Measurement and Modeling of Computer Systems*, pages 53–64, 2012.
- [9] Wei Bai, Li Chen, Kai Chen, Dongsu Han, Chen Tian, and Hao Wang. Pias: Practical information-agnostic flow scheduling for commodity data centers. *IEEE/ACM Transactions on Networking*, 25(4):1954–1967, 2017.
- [10] Hitesh Ballani, Paolo Costa, Raphael Behrendt, Daniel Cletheroe, Istvan Haller, Krzysztof Jozwik, Fotini Karinou, Sophie Lange, Kai Shi, Benn Thomsen, et al. Sirius: A flat datacenter network with nanosecond optical switching. In *Proceedings of the Annual conference of the ACM Special Interest Group on Data Communication on the applications, technologies, architectures, and protocols for computer communication*, pages 782–797, 2020.
- [11] Joshua L Benjamin, Thomas Gerard, Domaniç Lavery, Polina Bayvel, and Georgios Zervas. Pulse: optical circuit switched data center architecture operating at nanosecond timescales. *Journal of Lightwave Technology*, 38(18):4906–4921, 2020.
- [12] Kai Chen, Ankit Singla, Atul Singh, Kishore Ramachandran, Lei Xu, Yueping Zhang, Xitao Wen, and Yan Chen. Osa: An optical switching architecture for data center networks with unprecedented flexibility. *IEEE/ACM Transactions on Networking*, 22(2):498–511, 2013.
- [13] Kai Chen, Xitao Wen, Xingyu Ma, Yan Chen, Yong Xia, Chengchen Hu, and Qunfeng Dong. Wavecube: A scalable, fault-tolerant, high-performance optical data center architecture. In *2015 IEEE Conference on Computer Communications (INFOCOM)*, pages 1903–1911. IEEE, 2015.
- [14] Li Chen, Kai Chen, Zhonghua Zhu, Minlan Yu, George Porter, Chunming Qiao, and Shan Zhong. Enabling {Wide-Spread} communications on optical fabric with {MegaSwitch}. In *14th USENIX Symposium on Networked Systems Design and Implementation (NSDI 17)*, pages 577–593, 2017.
- [15] Shawn Shuoshuo Chen, Weiyang Wang, Christopher Canel, Srinivasan Seshan, Alex C Snoeren, and Peter Steenkiste. Time-division tcp for reconfigurable data center networks. In *Proceedings of the ACM SIGCOMM 2022 Conference*, pages 19–35, 2022.
- [16] Nathan Farrington, George Porter, Sivasankar Radhakrishnan, Hamid Hajabdolali Bazzaz, Vikram Subramanya, Yeshiahu Fainman, George Papen, and Amin Vahdat. Helios: a hybrid electrical/optical switch architecture for modular data centers. In *Proceedings of the ACM SIGCOMM 2010 Conference*, pages 339–350, 2010.
- [17] Monia Ghobadi, Ratul Mahajan, Amar Phanishayee, Nikhil Devanur, Janardhan Kulkarni, Gireeja Ranade, Pierre-Alexandre Blanche, Houman Rastegarfar, Madeleine Glick, and Daniel Kilper. Projector: Agile reconfigurable data center interconnect. In *Proceedings of the 2016 ACM SIGCOMM Conference*, pages 216–229, 2016.
- [18] Raj Joshi, Ben Leong, and Mun Choon Chan. Timer-tasks: Towards time-driven execution in programmable dataplanes. In *Proceedings of the ACM SIGCOMM 2019 Conference Posters and Demos*, pages 69–71, 2019.
- [19] Mehrdad Khani, Manya Ghobadi, Mohammad Alizadeh, Ziyi Zhu, Madeleine Glick, Keren Bergman, Amin Vahdat, Benjamin Klenk, and Eiman Ebrahimi. Sip-ml: high-bandwidth optical network interconnects for machine learning training. In *Proceedings of the 2021 ACM SIGCOMM 2021 Conference*, pages 657–675, 2021.
- [20] Erik Lambrechts, Annette MC Ficker, Dries R Goossens, and Frits CR Spieksma. Round-robin tournaments generated by the circle method have maximum carry-over. *Mathematical Programming*, 172:277–302, 2018.

- [21] Jeongkeun Lee. Advanced congestion & flow control with programmable switches. In *P4 Expert Roundtable Series*, 2020.
- [22] Yiming Lei, Jialong Li, Zhengqing Liu, Raj Joshi, and Yiting Xia. Nanosecond precision time synchronization for optical data center networks. *arXiv preprint arXiv:2410.17012*, 2024.
- [23] Jialong Li, Haotian Gong, Federico De Marchi, Aoyu Gong, Yiming Lei, Wei Bai, and Yiting Xia. Uniform-cost multi-path routing for reconfigurable data center networks. In *Proceedings of the ACM SIGCOMM 2024 Conference*, pages 433–448, 2024.
- [24] Jialong Li, Yiming Lei, Federico De Marchi, Raj Joshi, Balakrishnan Chandrasekaran, and Yiting Xia. Hop-on hop-off routing: A fast tour across the optical data center network for latency-sensitive flows. In *Proceedings of the 6th Asia-Pacific Workshop on Networking*, pages 63–69, 2022.
- [25] Cong Liang, Xiangli Song, Jing Cheng, Mowei Wang, Yashe Liu, Zhenhua Liu, Shizhen Zhao, and Yong Cui. Negotiator: Towards a simple yet effective on-demand reconfigurable datacenter network. In *Proceedings of the ACM SIGCOMM 2024 Conference*, pages 415–432, 2024.
- [26] He Liu, Feng Lu, Alex Forencich, Rishi Kapoor, Malveeka Tewari, Geoffrey M Voelker, George Papan, Alex C Snoeren, and George Porter. Circuit switching under the radar with {REACToR}. In *11th USENIX Symposium on Networked Systems Design and Implementation (NSDI 14)*, pages 1–15, 2014.
- [27] Hong Liu, Ryohei Urata, Kevin Yasumura, Xiang Zhou, Roy Bannon, Jill Berger, Pedram Dashti, Norm Jouppi, Cedric Lam, Sheng Li, et al. Lightwave fabrics: at-scale optical circuit switching for datacenter and machine learning systems. In *Proceedings of the ACM SIGCOMM 2023 Conference*, pages 499–515, 2023.
- [28] Yunpeng James Liu, Peter Xiang Gao, Bernard Wong, and Srinivasan Keshav. Quartz: a new design element for low-latency dcns. *ACM SIGCOMM Computer Communication Review*, 44(4):283–294, 2014.
- [29] William M Mellette, Rajdeep Das, Yibo Guo, Rob McGuinness, Alex C Snoeren, and George Porter. Expanding across time to deliver bandwidth efficiency and low latency. In *17th USENIX Symposium on Networked Systems Design and Implementation (NSDI 20)*, pages 1–18, 2020.
- [30] William M Mellette, Alex Forencich, Rukshani Athapathu, Alex C Snoeren, George Papan, and George Porter. Realizing rotornet: Toward practical microsecond scale optical networking. In *Proceedings of the ACM SIGCOMM 2024 Conference*, pages 392–414, 2024.
- [31] William M Mellette, Rob McGuinness, Arjun Roy, Alex Forencich, George Papan, Alex C Snoeren, and George Porter. Rotornet: A scalable, low-complexity, optical datacenter network. In *Proceedings of the Conference of the ACM Special Interest Group on Data Communication*, pages 267–280, 2017.
- [32] Behnam Montazeri, Yilong Li, Mohammad Alizadeh, and John Ousterhout. Homa: A receiver-driven low-latency transport protocol using network priorities. In *Proceedings of the 2018 Conference of the ACM Special Interest Group on Data Communication*, pages 221–235, 2018.
- [33] Matthew K. Mukerjee, Christopher Canel, Weiyang Wang, Daehyeok Kim, Srinivasan Seshan, and Alex C. Snoeren. Adapting TCP for Reconfigurable Datacenter Networks. In *17th USENIX Symposium on Networked Systems Design and Implementation (NSDI 20)*, pages 651–666, Santa Clara, CA, February 2020. USENIX Association.
- [34] George Porter, Richard Strong, Nathan Farrington, Alex Forencich, Pang Chen-Sun, Tajana Rosing, Yeshaiahu Fainman, George Papan, and Amin Vahdat. Integrating microsecond circuit switching into the data center. *ACM SIGCOMM Computer Communication Review*, 43(4):447–458, 2013.
- [35] Leon Poutievski, Omid Mashayekhi, Joon Ong, Arjun Singh, Mukarram Tariq, Rui Wang, Jianan Zhang, Virginia Beauregard, Patrick Conner, Steve Gribble, et al. Jupiter evolving: transforming google’s datacenter network via optical circuit switches and software-defined networking. In *Proceedings of the ACM SIGCOMM 2022 Conference*, pages 66–85, 2022.
- [36] Arjun Roy, Hongyi Zeng, Jasmeet Bagga, George Porter, and Alex C Snoeren. Inside the social network’s (datacenter) network. In *Proceedings of the 2015 ACM Conference on Special Interest Group on Data Communication*, pages 123–137, 2015.
- [37] Arjun Roy, Hongyi Zeng, Jasmeet Bagga, George Porter, and Alex C Snoeren. Inside the social network’s (datacenter) network. In *Proceedings of the 2015 ACM Conference on Special Interest Group on Data Communication*, pages 123–137, 2015.
- [38] Naveen Kr Sharma, Chenxingyu Zhao, Ming Liu, Pravein G Kannan, Changhoon Kim, Arvind Krishnamurthy, and Anirudh Sivaraman. Programmable calendar queues for high-speed packet scheduling. In *Proceedings of NSDI*, 2020.

- [39] John Von Neumann. A certain zero-sum two-person game equivalent to the optimal assignment problem. *Contributions to the Theory of Games*, 2(0):5–12, 1953.
- [40] Guohui Wang, David G Andersen, Michael Kaminsky, Konstantina Papagiannaki, TS Eugene Ng, Michael Kozuch, and Michael Ryan. c-through: Part-time optics in data centers. In *Proceedings of the ACM SIGCOMM 2010 Conference*, pages 327–338, 2010.
- [41] Weiyang Wang, Moein Khazraee, Zhizhen Zhong, Zhijiao Jia, Dheevatsa Mudigere, Ying Zhang, Anthony Kewitsch, and Manya Ghobadi. Topoopt: Optimizing the network topology for distributed dnn training. *arXiv preprint arXiv:2202.00433*, 2022.
- [42] Tegan Wilson, Daniel Amir, Vishal Shrivastav, Hakim Weatherspoon, and Robert Kleinberg. Extending optimal oblivious reconfigurable networks to all  $n$ . In *2023 Symposium on Algorithmic Principles of Computer Systems (APOCS)*, pages 1–16. SIAM, 2023.
- [43] Dingming Wu, Yiting Xia, Xiaoye Steven Sun, Xin Sunny Huang, Simbarashe Dzinamarira, and TS Eugene Ng. Masking failures from application performance in data center networks with shareable backup. In *Proceedings of the 2018 Conference of the ACM Special Interest Group on Data Communication*, pages 176–190, 2018.
- [44] Yiting Xia, Mike Schlansker, TS Eugene Ng, and Jean Tourrilhes. Enabling topological flexibility for data centers using omniswitch. In *HotCloud*, 2015.
- [45] Yiting Xia, Xiaoye Steven Sun, Simbarashe Dzinamarira, Dingming Wu, Xin Sunny Huang, and TS Eugene Ng. A tale of two topologies: Exploring convertible data center network architectures with flat-tree. In *Proceedings of the Conference of the ACM Special Interest Group on Data Communication*, pages 295–308, 2017.
- [46] Zhuolong Yu, Chuheng Hu, Jingfeng Wu, Xiao Sun, Vladimir Braverman, Mosharaf Chowdhury, Zhenhua Liu, and Xin Jin. Programmable packet scheduling with a single queue. In *Proceedings of the 2021 ACM SIGCOMM 2021 Conference*, pages 179–193, 2021.

## A Appendix

Table 5: Extra user API functions for *TA* architectures, the remaining ones are in Table 1.

Category	APIs	Description
<i>Topology</i>	<code>topo_aware(TM) → bool</code>	Abstract function to compute topology from traffic metric <code>TM</code> for the next update.
	↳ <code>bvn(TM), hotspot(TM), mip(TM)</code>	Circuit scheduling algorithms materializing <code>topo_aware()</code> .
<i>Routing</i>	<code>routing_aware() → [path(src,dst)]</code>	Abstract function to generate paths from <code>src</code> ToR to <code>dst</code> ToR.
	↳ <code>direct(), ecmp(), ksp()</code>	Routing algorithms materializing <code>routing_aware()</code> .
	<code>shortest_path(src,dst) → [path]</code>	Helper function returning the shortest paths from <code>src</code> ToR to <code>dst</code> ToR.